Exciton Lasing in ZnO-ZnCr$_2$O$_4$ Nanowalls

Tejendra Dixit
Jitesh Agrawal
Miryala Muralidhar
Masato Murakami
Kolla Lakshmi Ganapathi
Vipul Singh
M. S. Ramachandra Rao
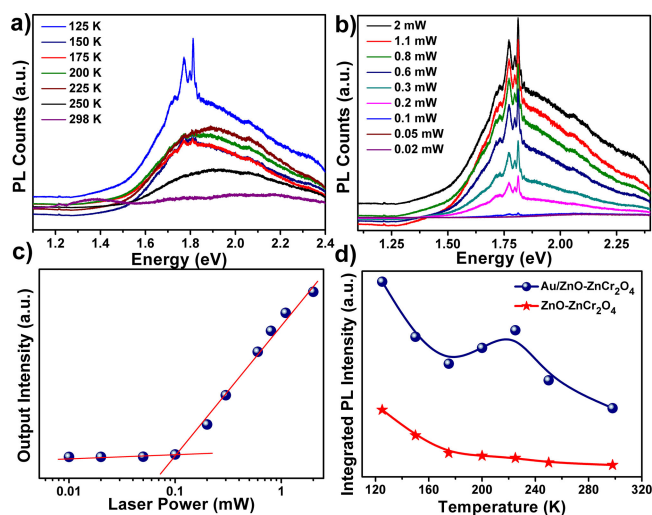
Exciton Lasing in ZnO-ZnCr$_2$O$_4$ Nanowalls

Tejendra Dixit [1,2] **Jitesh Agrawal** [3] **Miryala Muralidhar** [4]
Masato Murakami, [4] **Kolla Lakshmi Ganapathi** [1] **Vipul Singh** [3]
and M. S. Ramachandra Rao [1,2]

[1]Materials Science Research Centre and Department of Physics, Indian Institute of
Technology, Madras, Chennai 600036, India
[2]Nano Functional Materials Technology Centre, Indian Institute of Technology, Madras,
Chennai 600036, India
[3]Department of Electrical Engineering, Indian Institute of Technology, Indore,
Indore 453552, India
[4]Superconducting Material Laboratory, Graduate School of Science and
Engineering, Shibaura Institute of Technology, Tokyo 135-8546, Japan

Abstract: We demonstrate low power continuous wave, red and NIR exciton lasing with
FWHM of 1 nm, quality factor of 680 and threshold power of 100 μW in ZnO-ZnCr$_2$O$_4$
nanowalls. The NIR lasing was enabled by integrating ZnO with ZnCr$_2$O$_4$. Moreover, wave-
length selective photoluminescence (tuning from UV to NIR) and enhanced two-photon
emission were also observed in ZnO-ZnCr$_2$O$_4$ nanowalls. The exciton-exciton scattering
can be attributed to the observation of exciton lasing at low temperature ($<$200 K). A plausi-
ble mechanism has been elucidated in order to explain the results. This work will open new
opportunities in the advancement of oxide semiconductors based exciton lasers.

Index Terms: Photoluminescence spectroscopy, exciton-plasmon coupling, direct band
transition, multi-layer MoS$_2$.

1. Introduction

There are two major techniques of lasing i.e., conventional photon lasing and exciton and/or polari-
ton lasing. While, the threshold power is restricted by the population inversion of the electron-hole
plasma in the earlier, the scattering between excitons play significant role for the generation of
exciton lasing. In particular, pure exciton lasing has received substantial consideration in recent
years due to various reasons like sub-Mott density, low-threshold operation, etc.

ZnO is one of the most attractive semiconductor for the exploration of exciton lasing among sci-
entific community due to several factors like ease of fabrication, excellent optoelectronic properties
like high exciton binding energy (60 meV) etc. In the sequence to get room temperature exciton
lasing, ZnO microcrystals have been employed in recent years. R. Matsuzaki *et al.* have demon-

strated that pure exciton lasing i.e., lasing owing to exciton-exciton scattering is the dominating lasing mechanism from very low temperature to 150 K [1]. Moreover, they found that above 150 K the lasing process will be governed by exciton-electron or exciton-LO phonon scatterings. Y. Y. Lai *et al.* have also found that the exciton lasing is stable below 140 K in ZnO microcavity [2]. As far as the ZnO nanostructures are concerned realization of lasing due to exciton-exciton scattering is difficult to achieve at room temperature, which has been demonstrated by C. Klingshirn *et al.* [3], [4]. Here it must be noted that the exciton lasing has been explored for ZnO samples in the UV spectral region, only.

As ZnO is a potential contender for optoelectronic industry therefore, its applicability for visible and near infrared (NIR) region mainly for exciton lasing requires attention in order to compete with existing Si based technology [5], [6]. In sequence to get red and/or NIR emission in ZnO the typical technique is to dope a rare earth metal which makes the process complex and costly [7]. It is well known that Cr^{3+} ions are responsible for the red and NIR emission and have been used in various systems [8]. Although, Cr doping can systematically tune the emission properties of ZnO, however, hitherto there have been no reports on the realization of exciton lasing in Cr incorporated ZnO systems as has been observed in the present study. For the incorporation of Cr we have used our previous work in which we have observed that the integration of ZnO with ZnCr$_2$O$_4$ brings new functionality. Interestingly, neither ZnO nor ZnCr$_2$O$_4$ have shown any signature of red and NIR lasing, individually.

In this work, we demonstrate red and NIR exciton lasing in Au coated ZnO-ZnCr$_2$O$_4$ nanowalls. Systematic temperature dependent photoluminescence study has verified the involvement of exciton-exciton scattering at low temperatures (below 200 K). Here, it is important to note that the nanowalls configuration is required for achieving low threshold lasing. The formation of nanowalls in our case has helped to achieve low threshold lasing power density. Along with the NIR emission and low threshold operation another interesting feature is continuous wave (CW) mode operation. All the previous studies have used pump optical excitation to achieve exciton lasing in ZnO system. It is important to note that CW excitation has several advantages like low cost operation, better output stability etc. and therefore more focus on exciton lasing using CW excitation is needed [9]. This work will open new avenues in the field of pure exciton lasing.

2. Experimental Details

ZnO-ZnCr$_2$O$_4$ nanowalls were grown through solution process [10]. At first, ZnO seed layer (thin film) coating was done by spin coating a colloidal (stable) solution of zinc acetate, ethanolamine in 2-methoxyethanol on the pre-cleaned glass substrate. After that, seed layer coated samples were annealed at 250 °C in air for 5 minutes. Towards the nanowalls growth, the seed layer coated samples were kept at the bottom of the beaker filled with a solution prepared by mixing 0.1 M Zn(NO$_3$)$_2$. 6H$_2$O with equi-molar hexamethylenetetramine ((CH$_2$)$_6$N$_4$, also known as HMTA) in de-ionized (DI) water (25 mL). For the growth of ZnO-ZnCr$_2$O$_4$ nanowalls, 5 mM K$_2$Cr$_2$O$_7$ was added to the precursor solution. Finally, the beaker was sealed tightly and kept in an oven at 110 °C for 3 h for the uniform growth of the nanostructures. Finally, the samples were thoroughly washed with DI water to remove impurities [10]. For the analysis of emission spectra, the photoluminescence (PL) measurements were carried out using a continuous wave light source (λ value of 275 nm, 305 nm, 400 nm and 488 nm) from HORIBA LabRAM. In case of 488 nm laser; the laser spot size was nearly 1 μm. Time resolved PL measurements were done using Delta-Pro TCSPC Lifetime Fluorometer (HORIBA). Perkin Elmer (LAMBDA 950) spectrophotometer was used to record the UV-visible absorbance spectra (from 200 to 2500 nm range).

3. Results

Scanning electron microscope images of ZnO-ZnCr$_2$O$_4$ nanostructured film (recorded using FESEM-Zeiss Supra-55) is shown in Fig. 1(a). Formation of oriented nanowalls (average thickness of nanowalls were ~35 nm) can be clearly seen. The mechanism of nanowall growth is
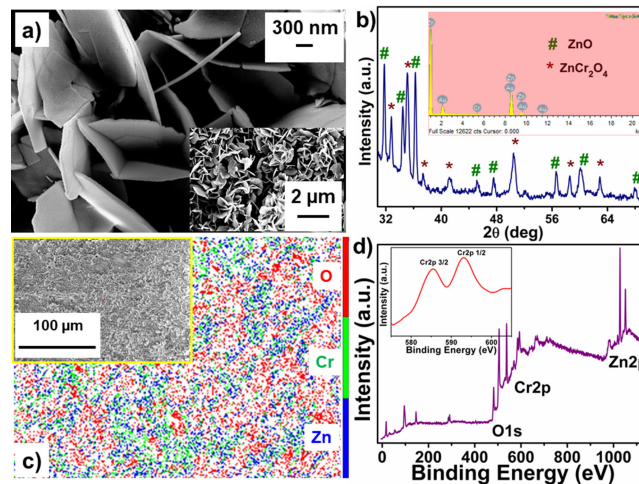
Fig. 1. (a) Scanning electron microscope image of ZnO-ZnCr$_2$O$_4$ nanowalls, inset shows the film morphology at low magnification; (b) X-ray diffraction patterns of the nanowalls, inset shows EDX spectra; (c) EPMA image (red, green and blue colors corresponds to Oxygen, Chromium and Zinc atoms, respectively); (d) High resolution X-ray photoelectron spectra.

mentioned in our previous work [10]. Concisely, addition of potassium dichromate plays a major role in the formation of nanowalls rather than typical nanorod structures. It was found that the nanowalls are broader at substrate and thin at the top i.e., making tapered nanowalls. The inset shows the morphology at low magnification. Powder-XRD (Rigaku Smart Lab system) plot for the nanowalls is shown in Fig. 1(b). Both, ZnO [ICDD#89–0510] and ZnCr$_2$O$_4$ [ICDD#22–1107] phases were clearly observed [11]. The electron dispersive spectrum (EDS) of Au/ZnO-ZnCr$_2$O$_4$ nanowalls is shown in the inset of Fig. 1(b), where all the elements can be clearly seen. For further investigating the elemental distribution, Electron Probe Micro Analyzer (EPMA) analysis was carried out using EPMA-JEOL: JXA-8530F system. EPMA results have shown that the elements were well distributed and thus it can be concluded that Cr is uniformly distributed in the matrix. The presence of Cr^{3+} ions in the matrix has been confirmed by high resolution XPS spectrum, which is shown in Fig. 1(d).

Fig. 2(a) shows the photoluminescence spectra of ZnO-ZnCr$_2$O$_4$ samples excited with three different wavelengths i.e., 275 nm, 305 nm and 400 nm. The PL spectra show a systematic modulation in the emission with the variation of excitation wavelength. In particular, with 275 nm excitation we were able to excite ZnCr$_2$O$_4$ phase with emission spectra encompassing UV, blue and green region of the electromagnetic spectra. The peak in the UV region i.e., between 320 nm-350 nm can be assigned to the direct band transitions of ZnCr$_2$O$_4$ [10]. With 305 nm excitation we were able to get broad emission covering UV, blue, green and orange spectral ranges. Interestingly, with 400 nm excitation we have observed strong blue-green and a signature of red emission. Visible region emissions are related to various defect related states of ZnO viz. oxygen vacancies (V$_o$), oxygen interstitials (O$_i$) etc. The visible region emissions can also be consigned to the several transitions associated to Cr^{3+} ions. Due to crystal field, the d-orbitals in the Cr^{3+} ions get split into t_2 and e-levels, thereby causing various transitions in the UV and visible region [12]. The similar trend has been reported in Si based devices and our results show that the ZnO-ZnCr$_2$O$_4$ nanowalls can also be used for visible and NIR emission [13], [14].

Interestingly, the sub-bandgap excitation (here, 488 nm laser has been used) shows amazing features i.e., NIR emission with peak position at 1.35 eV and 1.7 eV. Surprisingly, after Au coating we have found a significant enhancement in the NIR emission. The emission at 1.7 eV can be assigned to the typical 2E to ^{4}A$_2$ transitions in the Cr^{3+} ions. The 1.35 eV transition can be assigned to the band formation and low energy excitons associated with the 2E states. The time resolved PL spectra is shown in Fig. 2(c). Generally rare earth doped ZnO shows life time of μs
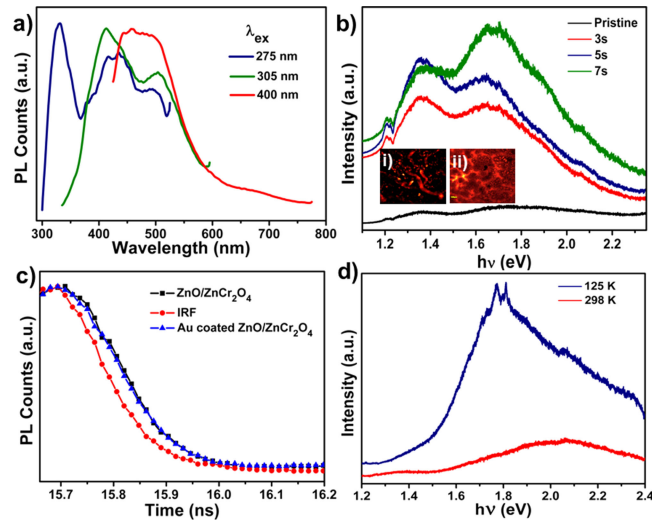
Fig. 2. (a) Room temperature PL spectra of ZnO-ZnCr$_2$O$_4$ nanowalls with various excitations; (b) PL spectra of Au coated ZnO-ZnCr$_2$O$_4$ nanowalls for different Au sputtering time (excited with 488 nm laser source), the inset show two-photon emission image (excited with 800 nm) of (i) ZnO-ZnCr$_2$O$_4$ nanowalls, (ii) Au/ZnO-ZnCr$_2$O$_4$ nanowalls; (c) Time resolved PL spectra; (d) PL spectra of pristine ZnO-ZnCr$_2$O$_4$ nanowalls at 298 K (red curve) and 125 K (blue curve).
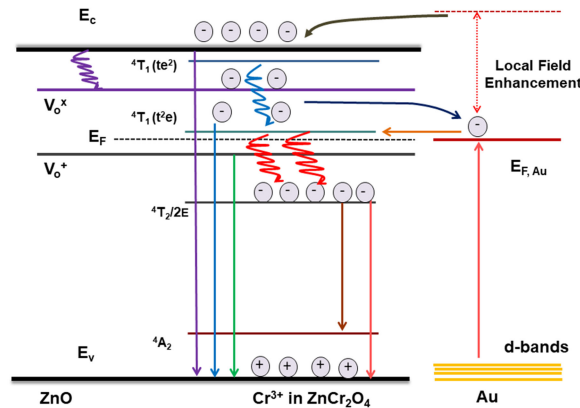

Fig. 3. Schematic for the charge transfer due to Au incorporation and energy levels responsible for emission.

while in our case it is in the range of several ps, which clearly suggests the involvement of excitonic transitions [1]. It must be noted here that, wiggles were perceived in the PL spectra for the Au coated samples. The intensity of PL was observed to increase with Au sputtering time and found to start decrease with 10 seconds of sputtering. The observation of wiggles in the spectra motivated us to investigate more. In that regard, we have taken PL spectra of the pristine samples at low temperatures. A clear transformation in the PL line shape can be seen at 125 K with two distinct peaks (as shown in Fig. 2(d)). This corresponds to the red and NIR transition due to the typical 2E to ^{4}A$_2$ transitions in the Cr^{3+} ions. Pristine and Au/ZnO-ZnCr$_2$O$_4$ nanowalls have shown two-photon emissions also (excited with two-photons of 800 nm light source). Interestingly with Au coating the emission efficiency turned out to be more prominent in comparison to the pristine samples (shown in the inset of Fig. 2(b)). The charge transfer from Au to Cr^{3+} energy levels can be assigned to enhancement in NIR emission. The schematic for the energy levels of Cr^{3+} ions and interaction with Au is shown in Fig. 3.
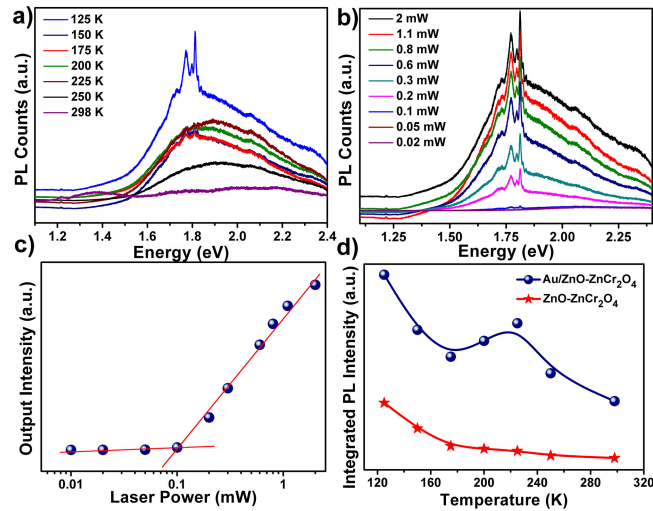
Fig. 4. Temperature dependent PL spectra of Au/ZnO-ZnCr$_2$O$_4$ nanowalls; (b) Excitation power dependent PL spectra of Au/ZnO-ZnCr$_2$O$_4$ nanowalls recorded at 125 K; (c) PL intensity vs. excitation power of Au/ZnO-ZnCr$_2$O$_4$ nanowalls recorded at 125 K. The lasing threshold has been estimated to be ~100 μW; (d) Integrated PL intensity versus temperature.

Temperature dependent PL spectra of Au/ZnO-ZnCr$_2$O$_4$ samples show several interesting features (shown in Fig. 4(a)). We can see that the two distinct peaks at 1.77 and 1.81 eV at 200 K and 150 K, which become dominant at 125 K with an additional sharp peak at 1.79 eV. The full width at half maximum (FWHM) for the peak in the red region was 1.3 nm and in the NIR region was 1.8 nm. The additional peak at 1.79 eV is however missing in pristine ZnO-ZnCr$_2$O$_4$ samples at 125 K and can be assigned to the interaction of Au with Cr^{3+} transitions and due to exciton-exciton scattering. The excitation intensity dependent PL spectra at 125 K were recorded and are shown in Fig. 4(b). Fig. 4(c) presents the excitation power dependent emission in the red and NIR region by varying laser power in the range 0.01 mW to 2 mW. It was found that the emission intensity increased abruptly beyond excitation power of 0.2 mW along with the emergence of sharp spike-like peaks. At lower excitation power (<0.2 mW), no such sharp peaks were observed. Such a low lasing threshold can be assigned to (a) exciton-exciton scattering process and (b) Nanowall morphology. Nanowalls with tapered thickness have been demonstrated by E. S. Jang et al. to produce lasing with very threshold power density [15]. Oriented nanowalls can serve as natural waveguide and thus invoke the lasing at low excitation powers. The improvement of internal reflection mostly at the top surface is helping to reach lasing with ease due to Au coating.

The lasing can be assigned either to excitonic process or electron-hole plasma (EHP) process, generally. It is well known that the EHP state is formed once the density of electron-hole pairs exceeds the critical value of Mott density defined as n_M. There is no shift observed in the peak position of any of the emissions with excitation power even at ~20 I_{ex}^{th}, which clearly discard the possibility of EHP process as a reason or the lasing [3]. From the temperature dependent PL spectra it is clear that lasing is happening below a certain temperature which is possible only due to exciton-exciton scattering. In case of exciton-exciton scattering typically, one exciton goes through radiative recombination, whereas the other exciton is scattered to higher excitonic states i.e., n = 2, 3, 4.....∞. Additionally, this exciton-exciton scattering induces stimulated emission. Moreover, the wall length (few microns) is more than the wavelength of emitted light, which means the structure can support the lasing. The transition from exciton-exciton scattering to exciton-electron scattering has been assigned for the observation of lasing action in ZnO microcrystals by Matsuzaki et al. with the variation of temperature [1]. They demonstrated that the value of $E_{ex}(T) - \hbar\omega_{max}^{obs}(T)$ follows different trends with temperature for exciton-exciton and exciton-electron scattering processes. Where, $E_{ex}(T)$ is the free exciton transition energy at a given temperature and $\hbar\omega_{max}^{obs}(T)$ is the peak
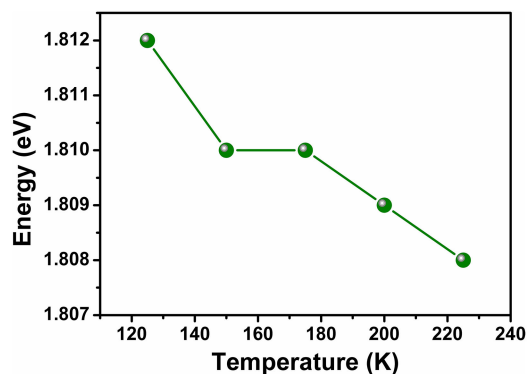
Fig. 5. Variation of $E_{ex}(T) - \hbar\omega_{max}^{obs}(T)$ with temperature.

energy as a function of temperature. In our case we have not observed any significant variation in the peak positions with temperature (the change in the peak present at 1.81 eV is nearly 4 meV even at 225 K to that of 125 K), which is shown in Fig. 5. These observations clearly suggest the presence of exciton-exciton scattering even at 225 K in Au/ZnO-ZnCr$_2$O$_4$ samples [1]. This system provides stable exciton-exciton scattering even at 200 K that can provide lasing.

The temperature-dependent integrated PL intensities of the pristine and Au coated ZnO-ZnCr$_2$O$_4$ nanowalls is shown in Fig. 4 (d). For pristine samples the plot follows Arrhenius formula, while for Au coated samples have shown a knee feature i.e., the intensity gradually increases as the temperature increases for a range of temperatures, which cannot be explained with Arrhenius formula [16], [17]. Similar trends have been shown by T. Lu *et al.* in case of GaN-based light-emitting diodes [17]. They have observed that the anomalous optical phenomenon is associated with the carrier transport behavior referred to as carrier mobility. Moreover, in case of optical excitation only, the observation of such an anomalous behavior is interesting. The temperature dependent charge transfer from Au to Cr^{3+} energy states and also the temperature dependent energy transfer from ZnO phase could play a role in this anomalous behavior. However, the origin of which is still under investigation.

4. Conclusions

Pure exciton lasing in red and NIR range has been shown in ZnO based system. Au coated ZnO-ZnCr$_2$O$_4$ nanowalls have been explored for various applications like red and NIR lasing and enhanced two-photon emission. The Au coated ZnO-ZnCr$_2$O$_4$ nanowalls have shown interesting feature of red and NIR lasing for the first time, which has been attributed to the exciton-exciton scattering at low temperature. We found that the exciton-exciton scattering is the leading effect for the lasing even at 225 K. ZnO-ZnCr$_2$O$_4$ system can be a potential candidate for exciton lasing and can further prompt the development of this field.

Acknowledgement

References

[1] R. Matsuzaki *et al.*, "Purely excitonic lasing in ZnO microcrystals: Temperature-induced transition between exciton-exciton and exciton-electron scattering" *Phys. Rev. B*, vol. 96, no. 12, Sep. 2017, Art. no. 125306.

[2] Y. Y. Lai, Y. H. Chou, Y. P. Lan, T. C. Lu, S. C. Wang, and Y. Yamamoto, "Crossover from polariton lasing to exciton lasing in a strongly coupled ZnO microcavity," *Sci. Rep.*, vol. 6, pp. 1–7, Feb. 2016.

[3] C. Klingshirn, R. Hauschild, J. Fallert, and H. Kalt, "Room-temperature stimulated emission of ZnO: Alternatives to excitonic lasing," *Phys. Rev. B*, vol. 75, no. 11, Mar. 2007, Art. no. 115203.

[4] M. A. M. Versteegh, D. Vanmaekelbergh, and J. I. Dijkhuis, "Room-Temperature laser emission of ZnO nanowires explained by many-body theory" *Phys. Rev. Lett.*, vol. 108, no. 15, Apr. 2012, Art. no. 157402.

[5] M. J. Chen *et al.*, "Stimulated emission in a nanostructured silicon pn junction diode using current injection," *Appl. Phys. Lett.*, vol. 84, no. 12, pp. 2163–2165, Mar. 2004.

[6] K. Xu *et al.*, "Light emission from a poly-silicon device with carrier injection engineering," *Materials Sci. Eng. B*, vol. 231, pp. 28–31, Apr. 2019.

[7] R. Khanum, R. S. Moirangthem, and N. M. Das, "Observation of defect-assisted enhanced visible whispering gallery modes in ytterbium-doped ZnO microsphere," *J. Appl. Phys.*, vol. 121, no. 2, May 2017, Art. no. 213101.

[8] M. García-Tecedor, D. Maestre, A. Cremades, and J. Piqueras, "Growth and characterization of Cr doped SnO$_2$ microtubes with resonant cavity modes," *J. Mater. Chem. C*, vol. 4, no. 24, pp. 5709–5716, May 2016.

[9] S Biswas and P. Kumbhakar, "Continuous wave random lasing in naturally occurring biocompatible pigments and reduction of lasing threshold using triangular silver nanostructures as scattering media," *Nanoscale*, vol. 9, no. 47, pp. 18812–18818, Nov. 2017.

[10] T. Dixit, I. A. Palani, and V. Singh, "Investigation on the influence of dichromate ion on the ZnO nano-dumbbells and ZnCr$_2$O$_4$ nano-walls," *J. Mater. Sci. Mater. Electron.*, vol. 26, no. 2, pp. 821–829, Nov. 2014.

[11] T. Dixit, J. Agrawal, K. L. Ganapathi, V. Singh, and M. S. R. Rao, "High-performance broadband photo-detection in solution-processed ZnO-ZnCr$_2$O$_4$ nanowalls," *IEEE Electron Device Lett.*, vol. 40, no. 7, pp. 1143–1146, Jul. 2019.

[12] T. Dixit, A. Kumar, I. A. Palani, and V. Singh, "Surface-plasmon-mediated red and near infrared emission from Au-coated ZnO/ZnCr$_2$O$_4$ nanocomposites," *Scr. Mater.*, vol. 114, pp. 84–87, Mar. 2016.

[13] C. H. Hsiao *et al.*, "Emitting layer thickness dependence of color stability in phosphorescent organic light-emitting devices," *Organic Electron.*, vol. 11, pp. 1500–1506, Jul. 2010.

[14] Kaikai Xu, "Silicon MOS optoelectronic micro-nano structure based on reverse-biased PN junction," *Physica status solidi a*, vol. 216, no. 7, Apr. 2019, Art. no. 1800868.

[15] E. S. Jang *et al.*, "Soft-solution route to ZnO nanowall array with low threshold power density," *Appl. Phys. Lett.* vol. 97, no. 4, Jul. 2010, Art. no. 043109.

[16] Z. F. Shi *et al.*, "Near-infrared random lasing realized in a perovskite CH$_3$NH$_3$PbI$_3$ thin film," *J. Mater. Chem. C*, vol. 4, no. 36, pp. 8373–8379, Aug. 2016.

[17] Z. Ma *et al.*, "Temperature-dependent photoluminescence in light-emitting diodes," *Sci. Rep.*, vol. 4, no. 6131, pp. 1–7, Aug. 2014.